SnailLoad: Exploiting Remote Network Latency Measurements without JavaScript

Stefan Gast, Roland Czerny, Jonas Juffinger, Fabian Rauscher, Simone Franza, and Daniel Gruss, *Graz University of Technology*

https://www.usenix.org/conference/usenixsecurity24/presentation/gast

This paper is included in the Proceedings of the 33rd USENIX Security Symposium.

August 14–16, 2024 • Philadelphia, PA, USA

978-1-939133-44-1

SnailLoad: Exploiting Remote Network Latency Measurements without JavaScript

Stefan Gast, Roland Czerny, Jonas Juffinger, Fabian Rauscher, Simone Franza, Daniel Gruss
Graz University of Technology

Abstract

Inferring user activities on a computer from network traffic is a well-studied attack vector. Previous work has shown that they can infer websites visited, videos watched, and even user actions within specific applications. However, all of these attacks require a scenario where the attacker can observe the (possibly encrypted) network traffic, e.g., through a person-in-the-middle (PITM) attack or sitting in physical proximity to monitor WiFi packets.

In this paper, we present SnailLoad, a new side-channel attack where the victim loads an asset, e.g., a file or an image, from an attacker-controlled server, exploiting the victim's network latency as a side channel tied to activities on the victim system, e.g., watching videos or websites. SnailLoad requires no JavaScript, no form of code execution on the victim system, and no user interaction but only a constant exchange of network packets, e.g., a network connection in the background. SnailLoad measures the latency to the victim system and infers the network activity on the victim system from the latency variations. We demonstrate SnailLoad in a non-PITM video-fingerprinting attack, where we use a single SnailLoad trace to infer what video a victim user is watching momentarily. For our evaluation, we focused on a set of 10 YouTube videos the victim watches, and show that SnailLoad reaches classification F_1 scores of up to 98 %. We also evaluated SnailLoad in an open-world top 100 website fingerprinting attack, resulting in an F_1 score of 62.8 %. This shows that numerous prior works, based on network traffic observations in PITM attack scenarios, could potentially be lifted to non-PITM remote attack scenarios.

1 Introduction

Side channels can leak information from implementations that are functionally correct and free of implementation errors [40]. Software-based side channels have gained an increasing amount of attention in the system security community, in particular cache attacks, which exploit timing differences induced by the caching infrastructure of a system [52, 79]. Software-based timing attacks, in particular on the cache, have been demonstrated on cryptographic algorithms [8], on ASLR (address-space layout randomization) [23, 31], secure enclaves [61], from websites [51], and to build covert channels [45, 59]. Most of these works study local scenarios where an attacker can execute native code [31], sandboxed code [77], or code run in an interpreter [62].

Other works study remote scenarios, typically with implementation-specific operations, such as encryption interfaces [10] or special hardware interfaces [42]. A more extensive set of works focuses on fingerprinting [65] using remote side channels, e.g., via passive traffic analysis from within the same network [7, 47, 70, 71]. Alexander and Crandall [4] focused on a more active attack scenario with spoofed SYN packets, triggering interaction between victim and server that the attacker can passively observe. Most works in this space, however, focus on person-in-the-middle scenarios to fingerprint, e.g., applications [69, 74] or websites [9, 58]. That is, they assume that the attacker controls at least one gateway or router in the path between server and victim. Naturally, this allows to monitor precise transmission times of packets, as well as their types and sizes [2,16,17,26,29,38,39,41,54,66,67,72]. Passive remote attacks have so far only been demonstrated in the context of the Tor anonymity network [46, 48]. Murdoch and Danezis [48] showed that they can reconstruct the activity of a Tor relay node using passive latency measurements.

Given this prior work we ask the following question: *Can a passive remote attacker use latency measurements as a side channel for browsing activity on a victim system? Can such a side-channel attack be mounted over the Internet?*

In this paper, we answer both questions in the affirmative: We show that neither specific code on the victim machine nor direct observation of the possibly encrypted network traffic is required to infer browsing activity on the victim system. We show that these attacks are possible from arbitrary Internet servers, with distances of more than 8 hops to the victim, and with only minimal network activity. SnailLoad exploits the subtle variations in the round-trip times (RTTs) of net-

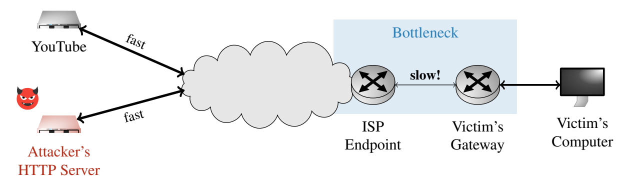

Figure 1: The attack setup for SnailLoad. A victim downloads data from an attacker's HTTP server while it watches a video on a video-sharing platform, e.g., YouTube. Due to the network bottleneck on the victim's side, the attacker can infer the transmitted amount of data by measuring the packet round trip time. The round trip time traces are unique per video and can be used to classify the video watched by the victim.

work packets that carry a side-channel signal influenced by activity of the victim. This enables an attacker to perform network side-channel attacks, that so far required a person-in-the-middle (PITM) scenario, from a fully passive and fully remote scenario off the transport path between victim and server.

We investigate the latency variations by analyzing the RTTs for different internet connections. Our analysis shows that the root cause of SnailLoad are bandwidth differences in the transport path between victim and server. As the server cannot know how fast the victim can receive the packets, it sends a certain amount (*i.e.*, a burst) of data in a short time frame. If there is a node on the transport path that hands over data from a higher bandwidth channel to a lower bandwidth channel, it has to buffer packets to transmit them sequentially over the lower bandwidth channel. Extreme cases where buffering leads to unusually high latencies are known as the *bufferbloat* phenomenon. While bufferbloat has only been considered a quality-of-service issue so far, SnailLoad shows that the timing differences induced by this buffering are exploitable by any attacker that can send packets through the same network node to the victim. Importantly, this node is typically the last node connecting the victim exclusively to the internet, *i.e.*, all packets to and from a victim pass through this node.

We evaluate SnailLoad in the first fully remote, non-person-in-the-middle web activity fingerprinting attack. To remain stealthy and to evade widely-used firewall restrictions (e.g., ICMP ping messages being dropped), we masquerade our SnailLoad latency measurements as a slow HTTP transfer from an attacker-controlled web server. This HTTP transfer can be a background connection, e.g., for a messenger app, or a slow website component embedded (e.g., an advertisement, image, font, or style sheet) in an otherwise benign and responsive website. Importantly, SnailLoad runs no code, e.g., no JavaScript, on the victim system. We show that a single SnailLoad trace from this scenario suffices to infer what video a victim user is watching momentarily. For our evaluation, we focused on a set of 10 YouTube videos the victim watches, and reach classification F_1 scores of up to 98 %. We also evaluated SnailLoad in an open-world website fingerprinting attack, resulting in a macro-averaged F_1 score of 62.8 %. When using SnailLoad across connections, with training data from one connection applied to another, we still achieve an F_1 score of 40 % in a top-10 closed-world fingerprinting scenario.

We evaluate the general applicability of SnailLoad on 10 home internet connections using ADSL, FTTH, FTTB, LTE, and cable access technologies. With training data from the victim's internet connection over the top 10 YouTube videos, played for 90 s with Firefox, we achieve F_1 scores between 37 % on an FTTB connection and 98 % on an FTTH connection. Our evaluation shows variations in the accuracy between internet access technologies, depending on whether the last-mile transport medium is shared among multiple subscribers or not. We evaluate the attack performance for probing frequencies between 20 Hz to 5 000 Hz, resulting in 0.4 kB/s to 320 kB/s of network traffic, in relation to differently-sized network activity of the victim ranging from 512 B to 8 MB. Our results show that with a higher probing frequency, we can observe also smaller-sized network activity of the victim. However, below a size of 512 kB, we find no probing frequency that leaks the network activity reliably. This is most likely due to not causing sufficient traffic for a visible amount of contention on the packet queue before the last mile, resulting in no visible delay for the attacker's packets.

We conclude that numerous prior works on network side channels in PITM attack scenarios could potentially be lifted to a remote non-PITM attack scenario based on SnailLoad.

Contributions. We summarize our contributions as follows:

1. We present SnailLoad, a new side-channel attack exploiting latency variations of the victim's network connection measured by loading an asset from an attacker-controlled server; allowing to infer web activity of a victim.
2. We show that the root cause of the side channel is buffering in a transport path node, typically the last node before the user's modem or router, related to a quality-of-service issue called bufferbloat.
3. We show that SnailLoad works despite the blocking of ICMP echo packets, through a low-bandwidth background connection such as a slow download, slow loading image in a website, or a connection for a chat client.
4. We evaluate SnailLoad in a user study with 10 different internet connections and 6 different connection technologies, achieving video-fingerprinting F_1 scores of 37 % to 98 %. We also evaluate SnailLoad in a top-100 open-world website-fingerprinting attack, achieving an F_1 score of 62.8 %.

Outline. Section 2 provides background on internet technologies and remote fingerprinting side-channel attacks. Section 3 presents the basic latency measurements that are the foundation of SnailLoad. Section 4 examines the root cause of SnailLoad. Section 5 presents the threat model and attack setup of SnailLoad. Section 6 evaluates SnailLoad in a video-fingerprinting scenario. We performed a user study comprising 10 different internet connections and 6 different internet connection technologies. Section 7 presents a top-100 open-world website-fingerprinting attack. We discuss the impact of SnailLoad and the relevant scenarios in Section 8. We conclude in Section 9.

2 Background

We provide background on internet access technologies typically used by end users to connect to the internet. Furthermore, we briefly introduce TCP/IP networking and dynamic adaptive streaming over HTTP. Finally, we describe video fingerprinting attacks and remote timing side channels.

2.1 Internet Access Technologies

While fast backbone internet routers deliver 100 Gbit/s per trunk line [24], with a recently ongoing shift to 400 Gbit/s technology [15], the last mile of an internet connection still forms a bandwidth bottleneck. For Q3 2023, a recent study [37] of an internet speed test provider shows a worldwide median download speed of 83.95 Mbit/s for wired connections and a worldwide median download speed of 203.04 Mbit/s for 5G connections, with high variations between different countries.

The prevalent connection types for end-users are DSL, cable, fiber optic, and mobile. In this section, we briefly describe their characteristics.

Digital Subscriber Line (DSL) DSL is an internet connection technology utilizing existing copper telephone lines. Multiple subscribers are connected to a DSL access multiplexer (DSLAM) before forwarding the connection to the internet service provider (ISP). The location of the DSLAM is an essential factor in the achievable bandwidth due to signal attenuation increasing with the length of the copper lines [21].

DSL has a low bandwidth and high latency compared to other technologies like cable and fiber optics. Download bandwidths typically range from 5 Mbit/s to 120 Mbit/s, with upload bandwidths from 1 Mbit/s to 20 Mbit/s. Since the last mile of DSL is shared between multiple participants, the bandwidth can be limited when many participants use the shared line. This also influences the latency.

Cable Similarly to DSL, cable internet also takes advantage of existing infrastructure: the coaxial cables for cable television. The Data Over Cable Service Interface Specification (DOCSIS) is a set of specifications standardizing data transmission over television cable systems [32]. In contrast to DSL, the length of the data cable, due to being a coaxial cable, is not that influential on the bandwidth.

However, the number of end users sharing the same connection strongly influences the bandwidth. The download bandwidth of cable internet is up to 10 Gbit/s with DOCSIS 4.0, and the upload bandwidth is up to 6 Gbit/s [32].

Fiber optic Fiber optic internet connections use light impulses transmitted via a fiber optic cable. They provide the highest bandwidth and lowest latency for data transmission, reaching up to 50 Gbit/s symmetric [19]. The fiber optic cable itself does not constrain this bandwidth but instead by the capabilities of the terminal equipment [56].

Fiber optic internet connections vary based on the composition of the last mile's connectivity. In a fiber-to-the-home (FTTH) setup, the entire last mile exclusively uses fiber optic cables, resulting in a non-shared, highly efficient connection.

In different, less costly configurations, such as Fiber-to-the-Curb (FTTC) or Fiber-to-the-Building (FTTB), existing infrastructure like coaxial cables links homes to the optical fiber network. In many instances, this leads to sharing lines with other users, similar to cable and DSL connections.

Mobile In contrast to the previously described wired technologies, the router is wirelessly connected to a cellular tower for a mobile internet connection. Because they generally serve multiple clients, the last mile of the connection is inherently shared, making the bandwidth and quality of the connection highly dependent on the number of clients.

The 5G standard uses higher frequency bands to increase bandwidth and reduce latency compared to 4G. Due to the higher frequency, 5G towers can only serve a smaller area than 4G towers. This leads to fewer users sharing the last mile, improving signal quality due to reduced congestion.

The bandwidth of 4G is up to 150 Mbit/s for download and up to 50 Mbit/s for upload. 4G+ increased it to 300 Mbit/s and 150 Mbit/s respectively [55]. 5G can reach significantly higher bandwidths, with up to 20 Gbit/s for download and 10 Gbit/s for upload [33].

2.2 TCP/IP Networking

The Transmission Control Protocol (TCP) is a protocol ensuring the correct and ordered transmission of data over a network. It works closely with the Internet Protocol (IP) that enables the transmission of packets across network boundaries from a specific source to a receiver. TCP/IP, the combined suite, forms the foundation of most modern internet communications, supporting a wide array of applications like web browsing (HTTP), E-Mail, and file transfers.

Packet Acknowledgment TCP is a connection-oriented protocol, using a handshake mechanism to establish a connection between sender and receiver. Upon the arrival of a packet, the receiver sends an acknowledgment packet (`ACK`) back to the sender, enabling the retransmission of lost packets.

TCP is implemented using send and receive buffers. Packets reside in the send buffer until an `ACK` is received. The size of the send buffer determines how many not-yet-acknowledged packets can be in transit. A receive buffer holds all received packets the application still needs to read.

Congestion Control Another vital feature of TCP is congestion control, which is crucial for maintaining a stable network, especially when it becomes heavily loaded. TCP employs several mechanisms to avoid or remove network congestion.

A congestion window determines the amount of data the sender may send before receiving an `ACK` packet. The size of the congestion window is controlled by the sender and is based on its perception of network congestion using information like lost or delayed `ACK` packets. The value adapts dynamically to the current load of the network.

To determine the congestion window size, typically, an algorithm known as *slow start* is employed. The initially small congestion window size is doubled upon each successful round trip until it reaches a threshold where packet loss is detected. Once the threshold is reached, TCP transitions from *slow start* to *congestion avoidance*. In this mode, the window size is changed more slowly to avoid congestion.

2.3 Dynamic Adaptive Streaming over HTTP

Dynamic Adaptive Streaming over HTTP (DASH) is a standard for video streaming [35], used by multiple video streaming services, including YouTube [26,39]. DASH servers split videos into small chunks of typically 2–6 seconds, each with multiple quality levels, allowing the client to request each chunk on demand, dynamically choosing a suitable bitrate, based on the available bandwidth. Video codecs and streaming services typically use variable-bitrate (VBR) encoding [6], enabling them to save bandwidth for scenes with only minor picture changes and to increase the bitrate for scenes containing more motion. Consequently, timing and sizes of transferred chunks differ for each video, based on the content.

2.4 Video Fingerprinting Attacks

As the timings and sizes of the transferred chunks form an individual fingerprint of each video, an attacker can infer the video played from the victim's network traffic by matching the observed traffic metadata against prerecorded traces. Multiple prior video fingerprinting attacks monitored network traffic directly from a PITM position [16,26,27,38,39] or from a WiFi signal [16]. More recent work [57] demonstrated a video fingerprinting attack based on the detection of network interrupts on the victim machine, indirectly observing network traffic. Inferring videos from traces is a typical classification task. Prior attacks used different classification methods, such as Dynamic Time Warping [26], Minimum Variance Matching [26], Nearest Neighbor Classification [16], Support Vector Machines [16], Sequential Minimal Optimization [39] or, more recently, convolutional neural networks [38,39,57].

2.5 Remote Timing Side Channels

In the context of side-channel attacks, the term *remote* has been used for a variety of scenarios. Some works described JavaScript-based attacks as *remote* [18,25,51,76], other attacks focus on specific interfaces, e.g., encryption interfaces or encrypted web traffic [8,10,13,14,63], and a third category of attacks works by only sending network packets to a machine without targeting specific interfaces [42,44,73]. All of these attacks rely on implementation-specific operations that the victim system performs that are unrelated to the actual victim activity targeted. Contention of buffers within the local (wireless) network [75] same system [20] can also contribute to performance anomalies that SnailLoad exploits.

In the context of IoT devices, passive traffic analysis from within the same network has been demonstrated to allow derivation of privacy-related information [7,47,71]. This is related to a line of research fingerprinting encrypted web traffic [65]. Previous works have demonstrated application fingerprinting [69,74], video fingerprinting [16,68], and website fingerprinting [9,58]. The two attack scenarios for these works are either a *local network attacker*, controlling a gateway in the local network far enough to spy on the traffic of a specific machine [7,47,70,71], or a *remote network attacker*, controlling a router somewhere in the path between server and victim. More active attacks can also trigger interaction between victim and server that the attacker then measures [4]. Different features that are available to such person-in-the-middle attackers have been exploited [2,16,17,26,29,38,39,72], e.g., message type [41,67], packet length [54,66]. Rather passive remote attacks have so far only been demonstrated in the context of the Tor network [46,48]. Murdoch and Danezis [48] showed that they can reconstruct the activity of a Tor relay node using passive latency measurements. Finally, many network side-channel works focus on the information recovery rather than the information collection aspect [9,16,58,68].

3 The Latency Side Channel

In this section, we **do not** yet mount an SnailLoad but only study the latency side channel. We examine latency variations on internet connections depending on different activities and show that the ISP's endpoint and the last mile have a significant influence. Our initial experiments also show that the effect can be observed by any unauthorized and unprivileged third party with a network connection to the system.

For now, we measure latencies using ICMP pings. For our SnailLoad attack later on, we have to resort to other packets as networks today commonly filter "ping packets" by default.

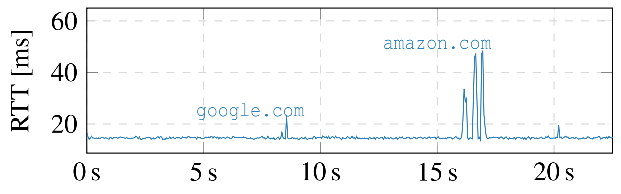

(a) Same machine pinging `8.8.8.8`.

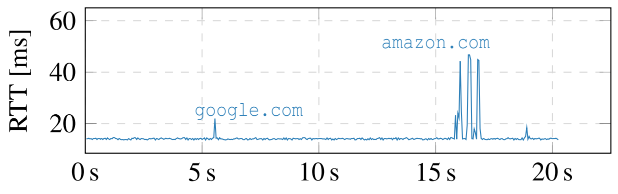

(b) Different machine in the same network pinging `8.8.8.8`

Figure 2: Effect of internet connection activity on the round trip times. A machine is constantly pinging `8.8.8.8` while the two websites `google.com` and `amazon.com` are opened. The internet is provided by a 50 Mbit/s ADSL connection.

The `ping` command sends an *ICMP Echo Request* to the target machine, which in turn responds with an *ICMP Echo Reply*. The latency between sending the ICMP Echo Request and receiving the ICMP Echo Reply is recorded as the *round trip time (RTT)*. Typical use cases of the `ping` command focus on the round trip time, e.g., to monitor the network status.

For our first experiment, we use a 50 Mbit/s ADSL connection, with a client machine directly connnected to the internet gateway (*i.e.*, home router) via an Ethernet cable. On the client machine, we `ping` the Google DNS server (IP: 8.8.8.8) with an interval of 50 ms and record the RTTs over time. Accessing `google.com` and `amazon.com` on the same machine shows RTT spikes while loading (cf. Figure 2a). We can see that this effect is quite subtle for a comparably plain website like the Google start page, while it is more noticeable for more complex websites like the Amazon start page. This is a surprising observation as either of the websites only triggers a few hundred kilobytes of traffic, nothing that should affect the network response times in a significant way.

The latency is influenced by small degrees of victim internet activity already.

In a second experiment, we show that the latency spikes are not caused by an effect on the client computer, e.g., kernel- or user-level packet handling, or system activity due to rendering. We repeat the experiment on the same internet connection but on a second machine directly connected to the gateway. We still `ping` the server from the first machine but load the websites on the second machine. This experiment results in the same latency spikes as shown in Figure 2b. This observation shows that the effect is not caused by any hardware or software component of either of the two client computers.

The latency is influenced by internet activity on other systems in the same network.

We also verify that the effect is not caused by the network connection between the two client machines. For this, the first client machine `ping`s the second machine, with the second machine loading the websites. In this scenario, we do not observe any latency spikes corresponding to website loads. We repeat the same experiment with a `ping` interval of 10 ms, again without observing latency spikes. The average RTT in this setting is 0.91 ms ($n = 2\,223$), with a maximum of only 1.5 ms at the start of the measurement, unrelated to the website loads. These results indicate that the observed latency spikes are caused by either the ISP's endpoint, the home internet gateway, or the last mile in between.

The latency is influenced by the ISP's endpoint and the last mile.

4 Latency Side Channel Root Cause Analysis

In this section, we analyze the root cause for the latency spikes observed in Section 3. We show that these can be explained by packet buffering at the ISP's endpoint, to which the customer's internet gateway is connected on the last mile.

As the last mile of the user's internet connection has a significantly lower bandwidth than backbone internet infrastructure (see Section 2.1), there is a bandwidth bottleneck at the ISP's endpoint (*i.e.*, DSLAM, CMTS, ONT, or cell tower). Network components, such as switches and routers, connect a high-bandwidth to a low-bandwidth network segment and buffer packets to be forwarded to the low-bandwidth segment. This prevents packet loss when the low bandwidth segment is congested. However, as packets have to be forwarded sequentially, a busy low-bandwidth connection delays the delivery of packets coming from the high-bandwidth segments.

The root cause of the latency side channel is the buffering of packets in nodes between high-bandwidth and low-bandwidth network segments, often located directly before the last mile. Typically, all internet packets for a specific user have to pass through this node.

We investigate the extent of this delay for 11 internet connections by comparing their baseline and congested `ping` round-trip times (RTTs). We directly connect a client computer to the home internet gateway (*i.e.*, router) via a standard 1000BASE-T (ethernet) cable and `ping` the Google DNS server (IP address: `8.8.8.8`). To measure the baseline RTT, we perform the measurement while the connection is other-

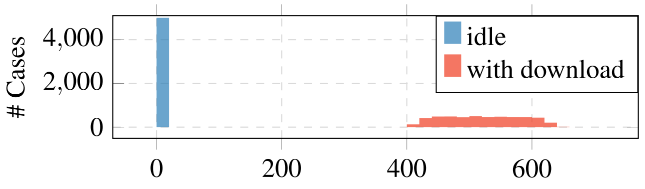

(a) Round trip time [ms] on ADSL-1 with 50 Mbit/s

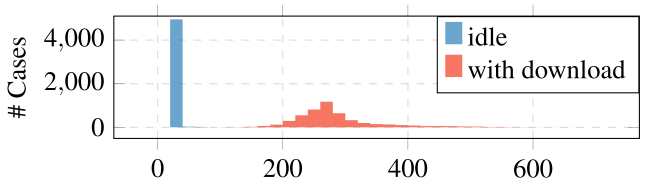

(b) Round trip time [ms] on LTE with 75 Mbit/s

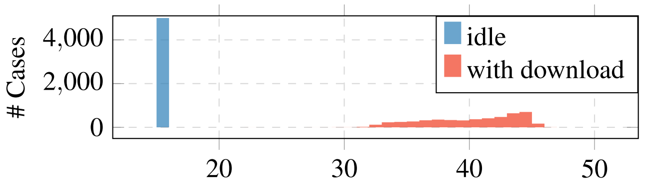

(c) Round trip time [ms] on FTTH-1 with 80 Mbit/s

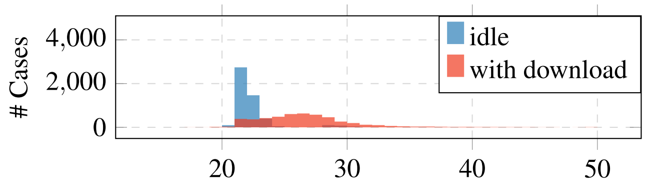

(d) Round trip time [ms] on Cable with 250 Mbit/s

Figure 3: Histograms of the round trip times of multiple internet connections, idle and with a download running in parallel.

Table 1: Tested internet connections and their round trip times (idle and saturated), as measured with ICMP Echo Requests.

Connection	Bandwidth [Mbit/s]		Idle RTT [ms]			Congested RTT [ms]		
	max.[1]	measured	min.	avg.	max.	min.	avg.	max
ADSL-1[2]	50	47	13.939	14.674	16.446	398.160	522.239	663.573
ADSL-2[2]	8	3.8	14.754	16.177	22.022	105.484	189.234	231.968
FTTH-1[2]	80	73.4	7.200	8.453	12.587	8.172	40.010	46.341
FTTH-2[3]	80	76.2	8	10.538	49	8	34.509	95
FTTH-3[2]	300	292.8	7.093	7.630	10.697	22.801	34.811	42.369
FTTB-1[4]	250	249	34.467	36.072	40.385	45.202	61.627	110.449
FTTB-2[2]	300	291.2	12.067	15.372	27.890	12.507	35.145	81.489
FTTB-3[2]	150	236.8	14.437	15.746	29.835	11.825	28.760	87.212
LTE[2]	75	78	49.683	52.844	56.483	156.945	322.248	588.891
LTE+[2]	200	120	30.515	34.329	77.128	40.969	293.244	815.692
Cable[2]	250	261.3	20.622	22.299	37.609	17.598	26.728	55.508

[1] according to ISP, [2] $n = 5000$ for RTT measurements, [3] $n = 1000$ for RTT measurements, [4] $n = 100$ for RTT measurements

wise idle. For the congested RTT, we perform the measurement while downloading a large file from a web server. We verify that the chosen download server has a transfer rate higher than the maximum download rate of the tested home internet connections by measuring its transfer rate at the university, where we measure a transfer rate of approximately 800 Mbit/s.

Our results, summarized in Table 1, show a substantial increase in the average RTTs for all the internet connections we tested. The histograms in Figure 3 show the distributions of the RTTs with and without a download running in parallel for an ADSL, an LTE, an FTTH, and a cable connection. Each of the internet connections we tested has characteristic distributions, showing that we are observing an effect specific to the internet connection itself.

Some of the tested connections show average RTTs of more than 150 ms when they are congested, such as the ADSL connections (ADSL-1 and ADSL-2 in Table 1) and the mobile connections (LTE and LTE+). These more extreme latency increases are caused by excessive buffering in network components, a networking problem known as bufferbloat [5, 20, 36]. While bufferbloat can be mitigated by Active Queue Management (AQM) schemes, such as CoDel [50, 64] or PIE [53], we want to emphasize that these only prevent excessive buffering and reduce the delay caused by it. Even with AQM schemes, the low-bandwidth bottleneck still exists, and some (reduced) form of buffering is required to prevent excessive packet loss. Thus, AQM reduces the difference in RTTs between an idle and a congested last mile. However, it cannot entirely eliminate the difference. Hence, all the tested connections carry a side-channel signal leaking usage information. Only for some of these connections, the side-channel signal is amplified by a heavy bufferbloat. Figure 4 illustrates the latency differences for idle, busy, and bufferbloat-affected connections.

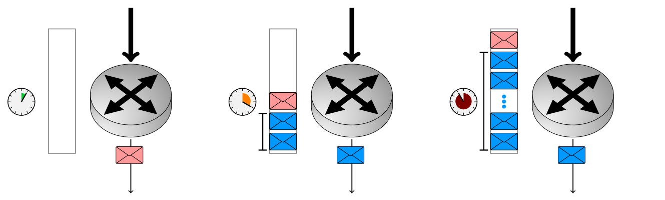

(a) Connection idle: packet forwarded immediately.

(b) Connection busy: packet buffered for a short delay.

(c) Bufferbloat: Excessive packets lead to long delays.

Figure 4: The effect of congestion on network latencies. The forwarding delay of the measurement packet correlates with the occupancy of the buffer in the router.

In extreme cases, the latency is amplified by the bufferbloat phenomenon.

While our analysis provides a good understanding of the latency side channel and the root cause of the latency variations and spikes, we now move on to the SnailLoad attack.

5 SnailLoad: Video-Fingerprinting Attack

In this section, we describe the SnailLoad attack in detail, starting with the threat model and attack overview. Because we cannot use `ping` to measure RTTs, we show a new accurate method to measure RTTs using TCP ACK packets. This method uses only 400 B/s of network traffic. Using it, we record network latency traces of streamed videos and classify them using a convolutional neural network. The average classification accuracy of 10 videos over all 10 tested internet connections is 66.8 %.

5.1 Threat Model

The attacker wants to know which video the victim user is watching. The attacker runs a native code TCP server and causes the victim to initiate a TCP connection with a download from the server while watching the video. As any background TCP transfer is enough to conduct SnailLoad, there are numerous ways to deploy it, e.g., download mirrors for legitimate benign software, (third-party) website assets like images, and several other scenarios (see Section 8). Importantly, the attacker cannot run any code on the victim machine, *i.e.*, the client application accessing the web server does not execute JavaScript or WebAssembly originating from the attacker's web server. We furthermore do not assume ICMP Echo Requests and ICMP Echo Responses to be forwarded between the victim and the attacker, *i.e.*, `ping` is blocked, a standard router configuration today [60].

Algorithm 1: Measuring round trip times using TCP Acknowledgment messages from a Linux process

```
Input: A socket descriptor sock with the
       TCP_NODELAY option set
Input: A single byte b to be sent to the client
Result: The measured round trip time rtt
begin
    acked ← false;
    start ← get_current_time();
    send(sock, b, 1, 0);
    repeat
        if ioctl(sock, SIOCOUTQ) = 0 then
            acked ← true;
        end
    until acked;
    end ← get_current_time();
    return end − start;
end
```

5.2 Attack Overview

Our video-stream fingerprinting attack consists of an online recording phase and an offline post-processing phase. During the recording phase, the attacking server records the network latency trace of the victim watching the first 90 seconds of a video, measuring the round trip times of single-byte TCP packets and their corresponding acknowledgment messages. In the post-processing phase, we infer which video was played from the recorded trace using a convolutional neural network trained with traces from an identical network setup.

5.3 Network Latency from TCP ACKs

In the previous experiments, we measured network round trip times using the `ping` command that was running on the victim machine. However, in our threat model, the attacker does not have control over the victim machine. We implement a similar measurement with code only running on the attacker-controlled server. While, in principle, it is possible to ping the public IP address of the victim machine, the attacker might not know the victim's public IP address in advance, and the internet gateway of the victim might be configured to drop ICMP echo requests for security reasons [60]. In this section, therefore, we exploit the TCP acknowledgment mechanism to measure round trip times, *i.e.*, any open TCP connection between victim and server is sufficient to record round trip times periodically.

5.3.1 TCP Packet Acknowledgments

To ensure reliable transmission, TCP requires the recipient to acknowledge each segment back to the server. For this, the receiver sends back a TCP message to the sender with the `ACK` flag and the acknowledgment number set in the TCP header (see Section 2.2). Measuring the time between sending some data and receiving the corresponding TCP acknowledgment again results in the round trip time, similar to using ICMP Echo Requests and Replies as before. However, unlike ICMP Echo Requests and Echo Responses, TCP acknowledgments are required for every TCP connection, and, therefore, they cannot be blocked globally.

> A single, low-traffic TCP connection is sufficient to mount SnailLoad. Blocking ICMP Echo messages does not prevent SnailLoad.

5.3.2 TCP Packet Acknowledgment Detection

Linux does not provide a standardized way to inform a user space application of packet acknowledgments. However, by probing the number of packets in the send buffer, we can see when a packet was acknowledged because it is removed from the send buffer. The equivalent information can also be obtained using *libpcap*, as we show in Section 7.

Algorithm 1 shows how such a measurement is implemented in a Linux server process. After obtaining the start time (Line 3), we invoke the `send` system call to enqueue a single byte to be transmitted to the victim machine (Line 4). As `send` returns immediately after placing the data to be sent in the send buffer, only timing the `send` system call is not sufficient. However, as described in Section 2.2, sent data is removed from the send buffer as soon as the server receives an acknowledgment for it. Consequently, in Line 5 until Line 9, we wait until the send buffer becomes empty again, using the `SIOCOUTQ` socket `ioctl` call to retrieve the number of bytes currently in the send buffer (Line 6). As soon as that number is 0 again, we leave the loop and obtain the end time in Line 10, yielding the round trip time as the difference between the end time and the start time (Line 11). Alternatively, an equivalent approach with *libpcap* can be used to match outgoing packets and incoming ACKs (cf. Section 7). For probing frequencies that may exceed the round-trip time of the connection, we resort to *libpcap*, and use the send buffer for lower frequency attacks (e.g., Section 6).

By setting the `TCP_NODELAY` socket option, we disable Nagle's Algorithm [34,49] to ensure that each of the single bytes is sent out immediately in separate TCP packets without merging multiple bytes into a single TCP packet. Consequently, each single byte is acknowledged separately by the victim machine. Therefore, each single-byte transmission enables the server to measure the round trip time to the victim. Furthermore, sending each byte in a separate TCP packet prevents measurement influence from changing TCP transmission window sizes.

> It is possible to detect TCP packet acknowledgments with user privileges by polling the TCP send buffer.

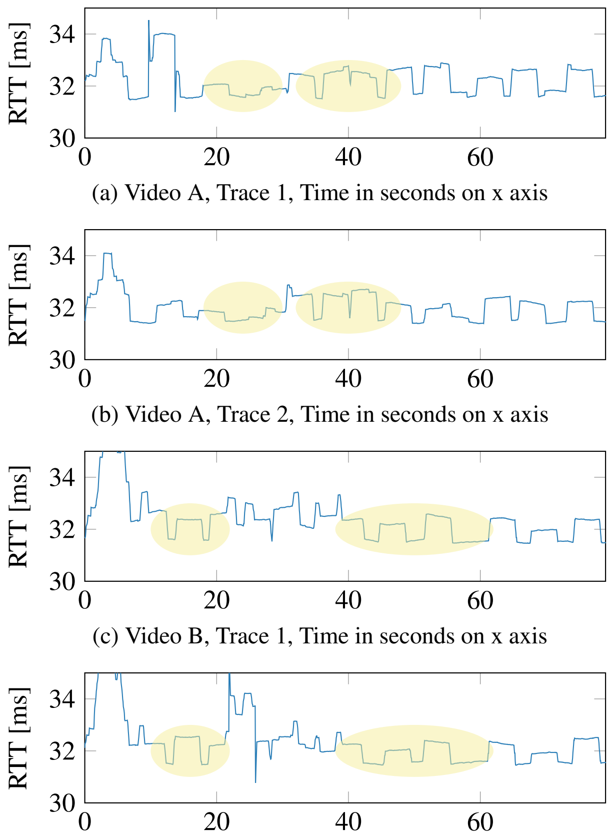

(a) Video A, Trace 1, Time in seconds on x axis

(b) Video A, Trace 2, Time in seconds on x axis

(c) Video B, Trace 1, Time in seconds on x axis

(d) Video B, Trace 2, Time in seconds on x axis

Figure 5: Averaged RTT traces from a client watching two different videos twice. There are features to distinguish the two videos and match the two traces of the identical videos.

5.3.3 Web Server Implementation

While SnailLoad works with any TCP connection, we implement a web server offering a file via HTTP to record network latency traces due to the large compatibility with existing client applications, *i.e.*, web browsers. The victim connects to the web server and requests the file. After sending back the HTTP header, the server performs latency measurements while transferring the file content. Every 50 ms, the server sends a single byte to the client and measures the round trip time by polling the send buffer, as previously described. We choose 50 ms as the time slice, since we want to have a high temporal resolution, yet we do not want to exceed the regular round trip time of an idle connection. This results in a low transfer rate of only $\frac{1\,\text{B}}{50\,\text{ms}} = 20\,\text{B/s}$ visible to the user, which gives SnailLoad its name. Effectively, due to the overhead of TCP/IP, this results in 400 B/s of network traffic, which is still very unsuspicious given that internet connections today can commonly handle multiple megabytes per second. Figure 5 shows the traces of one client watching two different videos two times. We can recognize the clear similarity between the

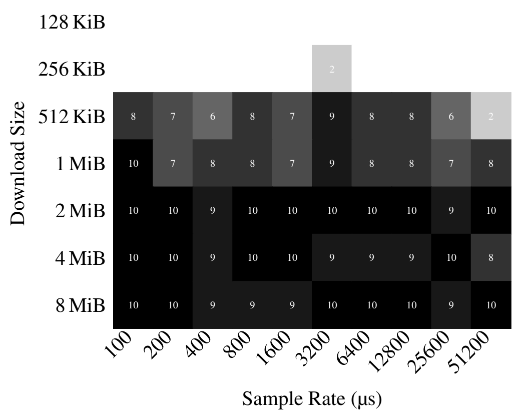

Figure 6: Identified downloads for different download sizes and sampling rates ($n = 10$). Evaluation with ADSL-1 (50 Mbit/s) connection.

same videos (traces 1 and 2) and see distinctive features for the other video (traces 3 and 4).

5.4 Attack Parameter Sweep

To determine the conditions under which the side channel works, we perform a parameter sweep, shown in Figure 6, with different download sizes and sample rates. The evaluation was done on the ADSL-1 (50 Mbit/s) connection. We evaluated sampling rates specified as window sizes between 100 µs, corresponding to 100 kHz, to 51 200 µs, corresponding to 19.5 Hz. Translating the connection capacity to these window sizes we obtain 336 kB per 51 200 µs and 655 B per 100 µs. Thus, in theory, transmitting as much data within this time frame should lead to contention in the buffer before the last mile and thus to a visible latency difference. However, as we see in Figure 6, even for higher sampling rates, we cannot reliably detect downloads of less than 512 kB. The reason for this may be that slow-start or congestion-avoidance mechanisms successfully prevent the negative impact of the download's packets on other packets. Furthermore, at higher sampling rates the TCP stack also starts grouping packets, effectively keeping the sampling rate higher than attempted. This observation can also be the reason for lower accuracies for some websites in our website-fingerprinting attack in Section 7.1, *i.e.*, due to their relatively low size.

5.5 Classifying Network Latency Traces with a Convolutional Neural Network

In order to efficiently classify the network latency traces, we employ a method typically used in signal classification [12, 30, 57, 78]. To classify a network latency trace, we first apply a Short-Time Fourier Transform (STFT) to it. An STFT performs multiple Fourier Transforms on short time windows of the network trace. The output of the STFT consists of two dimensions, with one dimension being the time and a second dimension being individual Fourier Transforms on the time slices, corresponding to the change in frequency over time. These two dimensions provide us with frequency information from the network trace while partially preserving the time domain. The 2D STFT allows us to perform convolutions on the data, which would not be directly possible with the initial one-dimensional network latency traces. We feed the output of the STFT into a convolutional neural network (CNN) for classification. We use KERAS (Tensorflow) on an Intel(R) Core(TM) i5-10210U CPU, with a runtime of 5 min to 10 min. The layout of the CNN is shown in Table 2. The CNN consists of three convolutional layers followed by three dense layers. The final layer outputs the likelihood that the input corresponds to a specific label for each possible label.

Table 2: CNN Parameters

Type	Parameters	Activation
Conv2D	filters=32, kernel size=[5,5], strides=[1,1]	ReLU
MaxPooling2D	pool size=[2,2], strides=[2,2]	-
Conv2D	filters=64, kernel size=[3,3], strides=[1,1]	ReLU
MaxPooling2D	pool size=[2,2], strides=[2,2]	-
Conv2D	filters=128, kernel size=[3,3], strides=[1,1]	ReLU
MaxPooling2D	pool size=[2,2], strides=[2,2]	-
Flatten	-	-
Dense	output size=1024	ReLU
Dense	output size=512	ReLU
Dense	output size=10	Softmax

6 SnailLoad: Video-Fingerprinting Evaluation

In this section, we show that SnailLoad leaks privacy-relevant information about which video a victim is playing. We evaluate SnailLoad on 10 different home internet connections. For a set of 10 YouTube videos, played for 90 s in Full HD resolution, our evaluation shows an accuracy of up to 98 %.

We select the videos in two steps: From the videos trending in the USA between October 2022 and September 2023, we first select the videos with at least 70 million views, yielding 23 videos. In the second step, we randomly select 10 videos out of this subset.

For each internet connection, we repeat the following three steps: First, we record 50 traces of the first 90 s of each of the 10 videos (Section 6.1). In the second step, we reserve a randomly selected subset of 10 traces per video as a test set and use the remaining 40 traces to train our CNN-based classifier (Section 6.2). Finally, we evaluate the trained model on the test set (Section 6.3).

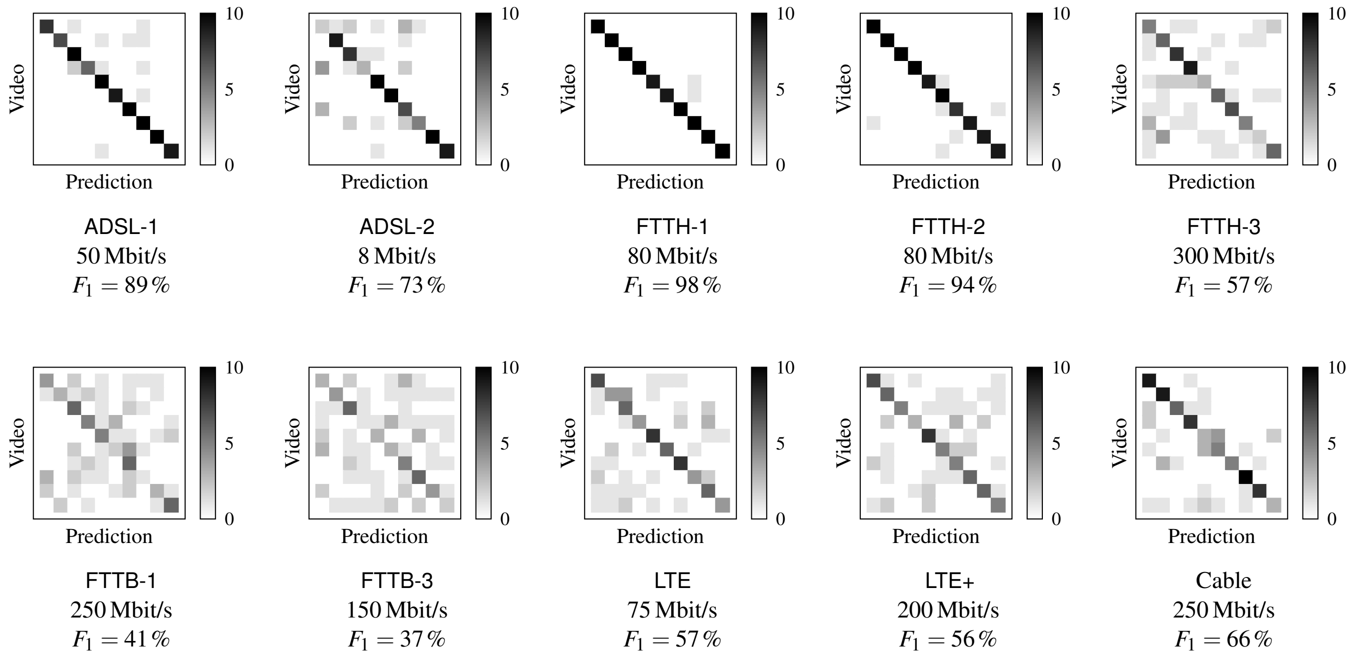

Figure 7: Confusion matrices for YouTube video fingerprinting on 10 internet connections.

6.1 Recording the Network Latency Traces

For each connection, we successively record traces for the 10 videos and repeat the recording in 2 batches with 25 iterations. Recording the videos successively during each iteration prevents correlations between daytime-dependent noise and the played video. For each trace, the client starts the SnailLoad HTTP file transfer and, after waiting for 3 s, also starts watching the video. After 90 s, the client aborts the file transfer and closes the video. After a pause of 3 s, the client continues with the next video. In total, recording all 500 traces for a single connection takes approximately 13.5 h.

Each recording is performed on one of two hosted servers, both of them connected to the Internet via a 1 Gbit/s downlink. Both servers are more than 8 hops away from the client machine, as tested with the `traceroute` command.

On the client machine, we use Firefox for both the HTTP file transfer and for watching the video. However, as the network-latency side channel is independent of the browser and operating system being used, we can expect similar results using another client configuration. We also tested this in smaller experiments but focused on this specific setup for the large-scale evaluation. As our traces shall only contain data from videos requested by the user, without any advertisements, we use uBlock Origin [28] as an ad blocker. Using an ad blocker is not strictly required for the attack because advertisements are effectively separate videos, and prior work [6] has shown that each video starts with a characteristic burst of network traffic, allowing the attacker to separate the advertisements from the video. However, it would increase the time until the video starts, prolonging the time the participants of our user study need to run the measurement. Hence, we opted for ad blocking to reduce the time for the participants.

6.2 Training the Classifier

After recording, we split the 50 traces of the 10 videos into training, validation and test sets. Following best practices [1], we use a training set of 36 traces per video to fit the model, a validation set of 4 traces per video to evaluate the model during training and a test set of 10 traces for the final evaluation of the trained model. For each internet connection, the individual hyperparameters for the CNN were empirically chosen to achieve good generalization against the validation set.

6.3 Results

After training the classifier for the internet connection, we evaluate the model on the test set. Figure 7 shows the results for all the 10 internet connections we tested. Each cell shows the probability that the classifier assigns the label indicated by the column to the videos indicated by the row. White or light gray cells indicate a low probability, whereas black or dark gray cells indicate a high probability. We also provide the F_1 scores we obtained for each connection.

For all the internet connections we tested, we obtain F_1 scores significantly better than random guessing (which would be $F_1 = 10\,\%$). The high probabilities along the diagonals in the confusion matrices also support that our attack works on all the tested connections. Overall, our F_1 scores range from 98 % for the FTTH-1 connection to 37 % for the FTTB-3 connection.

When comparing the FTTH connections, we notice a difference in accuracy between the 80 Mbit/s (FTTH-1, FTTH-2) and the 300 Mbit/s connection (FTTH-3). A lower bandwidth increases the transfer duration of the video segments, resulting in signal features that are easier to detect for our classifier. Thus, on the lower bandwidth FTTH-1 and FTTH-2 connections, we achieved accuracies of 98 % and 94 %, respectively, whereas on the higher bandwidth FTTH-3 connection, the accuracy was 57 %.

When comparing the results from the fiber-based connections, we notice a difference in accuracy between the FTTH connections and the FTTB connections. The accuracy with the FTTB-1 and FTTB-3 connections was significantly lower, with F_1 scores of only 41 % and 37 %, respectively. This might be caused by noise from other customers using the same shared fiber cable of the FTTB connection simultaneously. Especially for the FTTB-3 connection, when measuring the RTTs for the congested case in Section 4, we observed significant fluctuations in the measured latencies, which have a standard deviation of $\sigma = 12.595$ ms ($n = 5000$). This is relatively high when compared to the average RTT difference between the idle and congested case of only 13.014 ms, and thus makes detecting relevant features more challenging for the classifier.

Compared to the FTTB connections, we achieved higher accuracies on the cable and mobile connections. With the Cable connection, the accuracy was $F_1 = 66\,\%$. For the mobile LTE and LTE+ connection, we achieved similar F_1 scores of 57 % and 56 %, respectively. These comparatively high accuracies are surprising, as for both cable and mobile connections, the last mile is shared among multiple customers, similar to FTTB. However, both cable [32] and LTE [55] divide the frequency band used for transmissions into separate channels, possibly reducing the sharing between customers.

On both ADSL connections, we also achieved high accuracies of $F_1 = 89\,\%$ (ADSL-1) and $F_1 = 73\,\%$ (ADSL-2). The relatively low bandwidth contributes to prominent signal features (as shown in Figure 5) that improve the accuracy.

Overall, as with other fingerprinting attacks, the accuracy can be improved with more training data, *i.e.*, more or longer traces per video. However, we aimed to cover a wide variety of internet connections and recruited volunteers for recording the traces. While our recording time was limited for practical reasons, we assume that a dedicated attacker has the resources available to record more training data and thus to improve the accuracy of the attack even further.

We repeated the attack on the ADSL-1 connection, with the video quality reduced to 720p. On that connection, we have not observed any significant degradation in accuracy, even with the lower playback quality.

7 SnailLoad: Website-Fingerprinting

In this section, we present an open-world website-fingerprinting attack on the top 100 websites from the Alexa top 1 million list [3]. We use an *other* class for randomly sampled websites not in the top 100.

Threat Model and Attack Setup Our website-fingerprinting attack works in the same threat model as the video-fingerprinting attack in Section 6. The attacker wants to know which website the victim user opens while a background transfer is running a SnailLoad attack, *i.e.*, the online recording phase of the attack. The attacker still cannot run any code on the victim machine, *i.e.*, also no JavaScript. We again assume a standard router configuration [60], with ICMP Echo messages blocked. As most websites load within just a few seconds, we have to increase the attack sample rate to obtain a sufficient number of samples per trace. On the attacking download server, we therefore capture outgoing TCP packets and ingoing TCP ACKs using *libpcap* and compute the timings from the recorded packets, instead of using Algorithm 1. This allows us to increase the sample rate to 5 000 Hz, as we can now have multiple unacknowledged TCP packets in flight, without having to wait for each single packet to be acknowledged before sending the next packet. In an offline post-processing phase, we again use an STFT and a CNN-based classifier to identify the website visited by the victim. As we collect substantially more data, with a higher sample rate and more traces in total, we now use KERAS (Tensorflow) on an NVIDIA RTX 4080 GPU, with a runtime of 3 min to 7 min per training run. We also evaluate a cross-connection scenario, trained on one connection (ADSL-1) and applied to another (FTTH-1).

7.1 Evaluation

We evaluate our SnailLoad on in an open-world scenario. We collect 30 traces per classified website (3 000 in total). Since we evaluate an open-world scenario, we collect an additional `750` traces from randomly sampled from the Alexa top 1 million list [3], which are not in the top 100. With 10 seconds per trace and about 6.5 seconds to switch between websites, this yields a data collection runtime of about 17 hours. We randomly split the data for each class into 5 equally large parts and perform a 5-fold cross-validation, while making sure that the test set never overlaps with the training set in the same run. Consequently, in the open-world scenario, test set traces of the *other* class belong to websites that the model has never seen during training. We train our CNN with a validation split of 10 % of the training set.

Our classifier achieved a macro-averaged F_1 score of 62.8 %. The confusion matrix is shown in Figure 8 and Table 3 in the appendix shows the results for all websites in detail. The color of each cell indicates the prediction probability

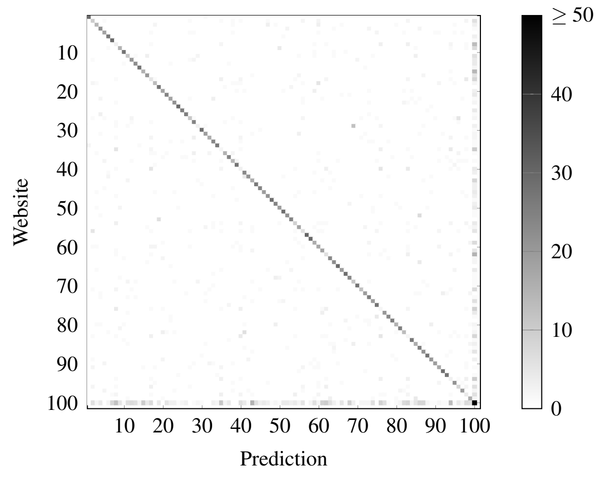

Figure 8: The confusion matrix for our top-100 open-world fingerprinting attack. The macro-averaged F_1 score is 62.8 %.

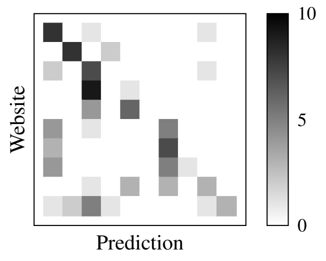

Figure 9: Training our neural network on connection ADSL-1 and applying the model to a trace from connection FTTH-1 yields a substantially higher accuracy than random-guessing, as visible with on the diagonal.

for each website, with a diagonal showing the high accuracy of our classifier across the vast majority of websites. The classification did not work well for 10 websites, resulting in F_1 scores below 20 %. These 10 websites include `wikipedia.org`, `t.co`, `yahoo.co.jp`, `jianshu.com`, which transfer less than 120 kB and thus are harder to detect for SnailLoad (see Figure 6). For `alipay.com` and `amazonaws.com`, we observe relatively slow loading times which may have moved the relevant features outside of our trace, which was restricted to only 10 seconds. All of the above websites had an F_1 score below 10 %. Four further websites had an F_1 score below 20 %, where `taobao.com`, `tmall.com`, and `cnki.net` were likely loading too slowly and `google.com.hk` was mostly misclassified as other Google domains. Excluding these websites, the macro-averaged F_1 score increases to 68.5 %. For 76 classes, including the *other* class, the F_1 score is above 50 %. The low performance for some websites is not surprising as different domains lead to the same actual page, e.g., Google domains are often misclassified as other Google domains.

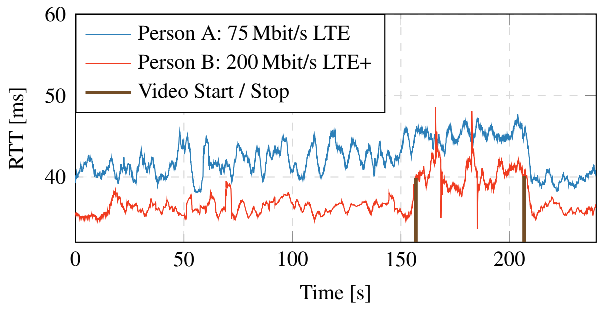

Figure 10: Detecting that two persons had a video call on Discord with each other. At around 155 s, the video call was started, resulting in an increase of RTTs on both connections. When the call ended at 205 s, the RTTs on both connections returned back to the lower baseline level.

In the cross-connection scenario, we apply a model trained on one connection (ADSL-1) to another connection (FTTH-1). We only performed a test on the top-10 websites in a closed-world scenario to minimize the time involvement for the participants of our study. In this scenario, we still achieve an F_1 score of 40 % (see Figure 9), which is significantly higher than random guessing.

8 Limitations and Discussion

While SnailLoad shows that obtaining a network latency trace of a victim system from only a TCP connection is feasible, inferring the specific web activity of the victim can be more challenging in practice. For our fingerprinting attacks, we used data from the same network connection for training set and test set. While we demonstrated in Section 7.1 that applying a model trained on one connection to a trace from another connection can yield a significantly higher accuracy than random-guessing, other scenarios may offer the possibility to obtain training and test data through the same network connection. This might be realistic if an attacker has access to the same network connection but in this situation the attacker likely already has other means than SnailLoad to observe the network latency, or even packet transmissions, of the victim. The attacker could also run the fingerprinting through a website, where one `iframe` shows the website of video to fingerprint, whereas another resource in the website is used to record a latency trace using SnailLoad. Consequently, the attacker has different means to obtain traces and mount an attack that can be adapted to the concrete setup and attacker capabilities. More generally, once SnailLoad leaked traces from a victim, an attacker can take arbitrary time to analyze or store the data until enough information is available to infer videos, websites, or other information contained in the trace.

In contrast to the remote timing side channels discussed in Section 2.5, which focus on JavaScript-based attacks or special network interfaces, SnailLoad is a *remote* attack in the sense that we do not rely on the victim system's own hardware or software implementation but contention of buffers that are in the transport path to the victim (close to the victim). SnailLoad is more similar to passive traffic analysis [7,47,71] but, in contrast to these works, does not require a person-in-the-middle attack scenario. SnailLoad instead can target any machine it can reach with a network connection. Gong et al. [22] already observed that ICMP ping times correlate with network activity on a DSL connection in 2010. However, ICMP ping packets are commonly blocked by default today [60]. In contrast to ICMP ping packets, the TCP ACKs used by SnailLoad are fundamental for reliable data transmission and cannot be blocked. Murdoch and Danezis [48] used passive latency measurements to estimate traffic on a Tor relay node. We go significantly beyond their attack and show that SnailLoad can infer specific videos a user watches on arbitrary network connections. In contrast to prior work focusing on information recovery, e.g., with deep-learning techniques [9,16,58,68], SnailLoad focuses on the information channel itself. Hence, SnailLoad could be combined with any of these works for generic non-person-in-the-middle information recovery, significantly amplifying the impact of these attacks.

To provide an example of such a use case of SnailLoad, we show that a scenario similar to the one explored by Li et al. [43] is also possible with SnailLoad. Instead of an instant messenger, we evaluate a video call scenario, where the attacker obtains latency traces of multiple victim systems and tries to infer which of these systems are interacting with each other, *i.e.*, which ones are having a joint video call. Figure 10 shows this for two persons having a short video call with each other on Discord, while the attacker records latency traces of both of them, as described in Section 5.3. The video call runs from $t = 155$ s to $t = 205$ s. The attacker observes a clear increase in RTTs for both victims in this specific time frame. Consequently, the attacker can deduce that they had a video call with each other in this time frame, again without requiring a PITM setting or the installation of stalkerware [11].

Mitigation of SnailLoad. Mitigating SnailLoad is not trivial as the root cause, the different bandwidths of channels in the transport path, cannot be eliminated. To provide adequate performance to multiple users simultaneously, the backbone network infrastructure has to have a higher bandwidth than the user's connection. Thus, the critical bottleneck is typically close to the user (*i.e.*, the last mile), and thus, the buffering occurs in a node that also handles the attacker's packets, even if packets have different priorities, e.g., due to quality-of-service measures. Dropping packets to avoid the bottleneck would not close the side channel, as the attacker could instead measure the share of dropped packets.

Similar as other side channels, SnailLoad is affected by noise and adding additional noise can hinder attacks. Noise is

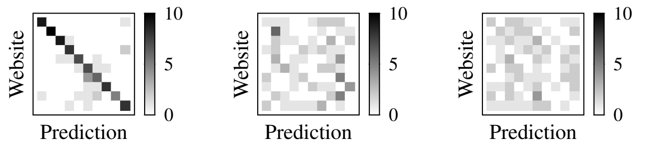

Figure 11: Adding noise on the FTTH-1 connection lets the fingerprinting accuracy deteriorate from an F_1 score of 77 % (left), to an F_1 score of 15 % when using noisy training and test sets (middle), and to an F_1 score of 10 % when using clean training and noisy test traces (right), which is the random-guessing probability.

added to contention side channels by adding spurious random contention. In our case, the contention comes from the last-mile bottleneck. Thus, we have to establish random traffic with an external server. We implemented a simple proof-of-concept that for every 5-second interval occupies the network connection randomly between 0 % to 100 %. To evaluate the effect of this noise on SnailLoad, we run a top-10 website-fingerprinting attack. Without noise, we achieve an F_1 score of 77 %, with a very clear diagonal visible in the confusion matrix in Figure 11. With noise, the F_1 score drops to 15 %, when using noisy traces for training and tests. This is just barely above the random-guessing probability and the diagonal does not stand out anymore. When using clean traces for the training, and noisy traces for the tests, the F_1 score drops even lower, to 10 %, which is the apriori probability of random guessing. This shows that noise can effectively mitigate SnailLoad. However, the noise also introduces an inconvenience for the user as it occupies part of the network connection.

Ethical Considerations. For our user study, we approached local undergraduate and graduate students who volunteered to run our measurement script. We asked the students not to perform any operations on the network that could expose personal information while running our script. Furthermore, it is essential to note that we only search for correlations between our measurements and the YouTube videos our measurements script opened. Thus, no personal information of the students was exposed to information leakage at any point. For the remaining possibility that students still used their network during the measurement time frame in a sensitive way, we are planning to destroy the traces after the publication of the paper and provide students with the option to ask us for the deletion of their traces and exclusion of their results from the paper at any point.

Responsible Disclosure. We demonstrated our video-fingerprinting attack on YouTube and, therefore, reported our attack to Google on March 9. Google acknowledged the severity and that it is a generic, unaddressed problem. For YouTube, they are investigating server-side mitigations.

9 Conclusion

While a substantial amount of research has studied person-in-the-middle side-channel attacks on encrypted web traffic, the possibility of such attacks in non-person-in-the-middle scenarios remained unclear. In this paper, we presented a novel attack, SnailLoad, that exploits the network packet latency as a side channel for activities on a victim system. Our root cause analysis indicates that buffering in a transport path node close to the victim is the root of the latency variations, as well as their connection to the bufferbloat quality-of-service phenomenon. We demonstrated SnailLoad in a scenario where the attacker hides the latency measurement in a network connection of the victim to retrieve an asset, e.g., a file or an image, from a seemingly benign attacker-controlled server. SnailLoad requires no JavaScript, no form of code execution on the victim system, no user interaction but only a constant exchange of network packets, e.g., a network connection in the background. We evaluated SnailLoad with a video-fingerprinting attack, inferring what video a user is watching from a single SnailLoad trace. Our user study comprised 10 internet connections with 6 different internet connection technologies. Over a set of the top 10 YouTube videos, we obtain classification F_1 scores between 37 % and 98 %. In a top-100 open-world website-fingerprinting attack, we achieve an F_1 score of 62.8 %. SnailLoad highlights that numerous prior works on network side channels could potentially be lifted to an non-PITM remote attack scenario.

Acknowledgments

We would like to thank our anonymous reviewers and our shepherd for their valuable and timely feedback. We furthermore thank David Bom, Lukas Maar, Sebastian Felix, Andreas Kogler, Lorenz Schumm, and Martin Glasner. This research was supported in part by the European Research Council (ERC project FSSec 101076409) and the Austrian Science Fund (FWF SFB project SPyCoDe 10.55776/F85 and FWF project NeRAM I6054). Additional funding was provided by generous gifts from Red Hat, Google, and Intel. Any opinions, findings, and conclusions or recommendations expressed in this paper are those of the authors and do not necessarily reflect the views of the funding parties.

References

[1] Akruti Acharya. Training, Validation, Test Split for Machine Learning Datasets, 2023. URL: https://encord.com/blog/train-val-test-split/.

[2] Waleed Afandi, Syed Muhammad Ammar Hassan Bukhari, Muhammad U. S. Khan, Tahir Maqsood, and Samee U. Khan. Fingerprinting Technique for YouTube Videos Identification in Network Traffic. *IEEE Access*, 10:76731–76741, 2022.

[3] Alexa Internet, Inc. The top 1 million sites on the web, 5 2024. URL: https://www.alexa.com/topsites.

[4] Geoffrey Alexander and Jedidiah R Crandall. Off-path round trip time measurement via TCP/IP side channels. In *IEEE International Conference on Computer Communications (INFOCOM)*, 2015.

[5] Mark Allman. Comments on bufferbloat. *ACM SIGCOMM Computer Communication Review*, 43(1):30–37, 2012.

[6] Pablo Ameigeiras, Juan J. Ramos-Munoz, Jorge Navarro-Ortiz, and J.M. Lopez-Soler. Analysis and modelling of YouTube traffic. *Transactions on Emerging Telecommunications Technologies*, 23(4):360–377, 2012.

[7] Noah Apthorpe, Dillon Reisman, Srikanth Sundaresan, Arvind Narayanan, and Nick Feamster. Spying on the smart home: Privacy attacks and defenses on encrypted iot traffic. *arXiv:1708.05044*, 2017.

[8] Daniel J. Bernstein. Cache-Timing Attacks on AES, 2005. URL: http://cr.yp.to/antiforgery/cachetiming-20050414.pdf.

[9] Sanjit Bhat, David Lu, Albert Kwon, and Srinivas Devadas. Var-CNN: A Data-Efficient Website Fingerprinting Attack Based on Deep Learning. *Proceedings on Privacy Enhancing Technologies (PoPETS)*, 4:292–310, 2019.

[10] David Brumley and Dan Boneh. Remote timing attacks are practical. *Elsevier Computer Networks*, 48(5):701–716, 2005.

[11] Rahul Chatterjee, Periwinkle Doerfler, Hadas Orgad, Sam Havron, Jackeline Palmer, Diana Freed, Karen Levy, Nicola Dell, Damon McCoy, and Thomas Ristenpart. The spyware used in intimate partner violence. In *IEEE Symposium on Security and Privacy (S&P)*, 2018.

[12] Zhibo Chen, Yi-Qun Xu, Hongbin Wang, and Daoxing Guo. Deep STFT-CNN for spectrum sensing in cognitive radio. *IEEE Communications Letters*, 2020.

[13] David Cock, Qian Ge, Toby Murray, and Gernot Heiser. The last mile: An empirical study of timing channels on seL4. In *ACM Conference on Computer and Communications Security (CCS)*, 2014.

[14] Scott A Crosby, Dan S Wallach, and Rudolf H Riedi. Opportunities and limits of remote timing attacks. *ACM Transactions on Information and System Security (TISSEC)*, 12(3):17, 2009.

[15] Dell'Oro Group. 400 Gbps Technology: The Next Phase of the Internet Backbone Expansion, 2022. URL: https://www.delloro.com/400-gbps-technology-the-next-phase-of-the-internet-backbone-expansion/.

[16] Ran Dubin, Amit Dvir, Ofir Pele, and Ofer Hadar. I Know What You Saw Last Minute—Encrypted HTTP Adaptive Video Streaming Title Classification. *IEEE Transactions on Information Forensics and Security (TIFS)*, 12(12):3039–3049, 2017.

[17] Saman Feghhi and Douglas J. Leith. A Web Traffic Analysis Attack Using Only Timing Information. *IEEE Transactions on Information Forensics and Security (TIFS)*, 2016.

[18] Edward W Felten and Michael A Schneider. Timing attacks on web privacy. In *ACM Conference on Computer and Communications Security (CCS)*, 2000.

[19] Ziply Fiber. 50 Gbit/s fiber optic internet, 2023. URL: https://web.archive.org/web/20240120003846/https://ziplyfiber.com/internet/multigig.

[20] Jim Gettys. Bufferbloat: Dark buffers in the internet. *IEEE Internet Computing*, 15(3):96–96, 2011.

[21] Philip Golden, Hervé Dedieu, and Krista S Jacobsen. *Implementation and Applications of DSL Technology*. CRC press. 978-0-8493-3423-8, 2007.

[22] Xun Gong, Negar Kiyavash, and Nikita Borisov. Fingerprinting Websites Using Remote Traffic Analysis. In *ACM Conference on Computer and Communications Security (CCS)*, 2010.

[23] Ben Gras, Kaveh Razavi, Erik Bosman, Herbert Bos, and Cristiano Giuffrida. ASLR on the Line: Practical Cache Attacks on the MMU. In *Network and Distributed System Security (NDSS) Symposium*, 2017.

[24] Tim Greene. What is the internet backbone and how it works, 2020. URL: https://www.networkworld.com/article/968484/what-is-the-internet-backbone-and-how-it-works.html.

[25] Daniel Gruss, Clémentine Maurice, and Stefan Mangard. Rowhammer.js: A Remote Software-Induced Fault Attack in JavaScript. In *SIG SIDAR Conference on Detection of Intrusions and Malware & Vulnerability Assessment (DIMVA)*, 2016.

[26] Jiaxi Gu, Jiliang Wang, Zhiwen Yu, and Kele Shen. Walls Have Ears: Traffic-based Side-Channel Attack in Video Streaming. In *IEEE International Conference on Computer Communications (INFOCOM)*, 2018.

[27] Jiaxi Gu, Jiliang Wang, Zhiwen Yu, and Kele Shen. Traffic-based side-channel attack in video streaming. *IEEE/ACM Transactions on Networking*, 27(3):972–985, 2019.

[28] Raymond Hill. uBlock Origin - An efficient blocker for Chromium and Firefox. Fast and lean., 7 2017. URL: https://github.com/gorhill/uBlock.

[29] Michael Augustus Hogye, Christopher Taddeus Hughes, Joshua Michael Sarfaty, and Joseph David Wolf. Analysis of the Feasibility of Keystroke Timing Attacks over SSH Connections. Technical report, School of Engineering and Applied Science University of Virginia, 2001.

[30] Jingshan Huang, Binqiang Chen, Bin Yao, and Wangpeng He. ECG arrhythmia classification using STFT-based spectrogram and convolutional neural network. *IEEE Access*, 7:92871–92880, 2019.

[31] Ralf Hund, Carsten Willems, and Thorsten Holz. Practical Timing Side Channel Attacks against Kernel Space ASLR. In *IEEE Symposium on Security and Privacy (S&P)*, 2013.

[32] CableLabs Inc. DOCSIS 4.0 Technology, 2023. URL: https://web.archive.org/web/20240108220840/https://www.cablelabs.com/technologies/docsis-4-0-technology.

[33] International Telecommunication Union. Report ITU-R M.2410-0: Minimum requirements related to technical performance for IMT-2020 radio interface(s), 2017. URL: https://ieg.5gindiaforum.in/docs/M.2410-TPR.pdf.

[34] Internet Engineering Task Force. RFC 1122: Requirements for Internet Hosts – Communication Layers, 1989. URL: https://datatracker.ietf.org/doc/html/rfc1122.

[35] ISO/IEC. Dynamic adaptive streaming over HTTP (DASH) (ISO/IEC 23009-1:2022), 2022.

[36] Haiqing Jiang, Yaogong Wang, Kyunghan Lee, and Injong Rhee. Tackling bufferbloat in 3G/4G networks. In *Internet Measurement Conference (IMC)*, 2012.

[37] Sylwia Kechiche. The State of Worldwide Connectivity in 2023, 2023. URL: https://www.ookla.com/articles/worldwide-connectivity-mobile-fixed-networks-digital-divide-2023.

[38] Muhammad U. S. Khan, Syed M. A. H. Bukhari, Tahir Maqsood, Muhammad A. B. Fayyaz, Darren Dancey, and Raheel Nawaz. SCNN-Attack: A Side-Channel Attack to Identify YouTube Videos in a VPN and Non-VPN Network Traffic. *MDPI Electronics*, 11(3), 1 2022.

[39] Muhammad US Khan, Syed MAH Bukhari, Shazir A Khan, and Tahir Maqsood. ISP can identify YouTube videos that you just watched. In *IEEE International Conference on Frontiers of Information Technology (FIT)*, 2021.

[40] Paul Kocher. Timing Attacks on Implementations of Diffe-Hellman, RSA, DSS, and Other Systems. In *Advances in Cryptology - CRYPTO: Annual International Cryptology Conference*. Springer, 1996.

[41] Maciej Korczyński and Andrzej Duda. Markov chain fingerprinting to classify encrypted traffic. In *IEEE Conference on Computer Communications*, 2014.

[42] Michael Kurth, Ben Gras, Dennis Andriesse, Cristiano Giuffrida, Herbert Bos, and Kaveh Razavi. NetCAT: Practical Cache Attacks from the Network. In *IEEE Symposium on Security and Privacy (S&P)*, 2020.

[43] Ke Li, Hong Li, Hongsong Zhu, Limin Sun, and Hui Wen. Side-channel information leakage of traffic data in instant messaging. In *International Performance Computing and Communications Conference (IPCCC)*, 2019.

[44] Moritz Lipp, Misiker Tadesse Aga, Michael Schwarz, Daniel Gruss, Clémentine Maurice, Lukas Raab, and Lukas Lamster. Nethammer: Inducing Rowhammer Faults through Network Requests. In *Security of Hardware Software Interfaces (SILM) Workshop*, 2020.

[45] Clémentine Maurice, Manuel Weber, Michael Schwarz, Lukas Giner, Daniel Gruss, Carlo Alberto Boano, Stefan Mangard, and Kay Römer. Hello from the Other Side: SSH over Robust Cache Covert Channels in the Cloud. In *Network and Distributed System Security (NDSS) Symposium*, 2017.

[46] Prateek Mittal, Ahmed Khurshid, Joshua Juen, Matthew Caesar, and Nikita Borisov. Stealthy traffic analysis of low-latency anonymous communication using throughput fingerprinting. In *ACM Conference on Computer and Communications Security (CCS)*, 2011.

[47] Nizar Msadek, Ridha Soua, and Thomas Engel. IoT device fingerprinting: Machine learning based encrypted traffic analysis. In *Wireless Communications and Networking Conference (WCNC)*, 2019.

[48] Steven J Murdoch and George Danezis. Low-cost traffic analysis of Tor. In *IEEE Symposium on Security and Privacy (S&P)*, 2005.

[49] John Nagle. RFC 896: Congestion Control in IP/TCP Internetworks, 1984. URL: https://datatracker.ietf.org/doc/html/rfc896.

[50] Kathleen Nichols and Van Jacobson. Controlling queue delay. *Communications of the ACM*, 55(7):42–50, 2012.

[51] Yossef Oren, Vasileios P Kemerlis, Simha Sethumadhavan, and Angelos D Keromytis. The Spy in the Sandbox: Practical Cache Attacks in JavaScript and their Implications. In *ACM Conference on Computer and Communications Security (CCS)*, 2015.

[52] Dag Arne Osvik, Adi Shamir, and Eran Tromer. Cache Attacks and Countermeasures: the Case of AES. In *Topics in Cryptology - CT-RSA: The Cryptographers' Track at the RSA Conference*, 2006.

[53] Rong Pan, Preethi Natarajan, Chiara Piglione, Mythili Suryanarayana Prabhu, Vijay Subramanian, Fred Baker, and Bill VerSteeg. PIE: A lightweight control scheme to address the bufferbloat problem. In *IEEE International Conference on High Performance Switching and Routing (HPSR)*, 2013.

[54] Andriy Panchenko, Fabian Lanze, Jan Pennekamp, Thomas Engel, Andreas Zinnen, Martin Henze, and Klaus Wehrle. Website Fingerprinting at Internet Scale. In *Network and Distributed System Security (NDSS) Symposium*, 2016.

[55] Stefan Parkvall, Erik Dahlman, Anders Furuskar, Ylva Jading, Magus Olsson, Stefan Wanstedt, and Kambiz Zangi. LTE-Advanced - Evolving LTE towards IMT-Advanced. In *IEEE Vehicular Technology Conference*, 2008.

[56] Benjamin J Puttnam, Ruben S Luís, Georg Rademacher, Yoshinari Awaji, and Hideaki Furukawa. 319 Tb/s Transmission over 3001 km with S, C and L band signals over >120nm bandwidth in 125μm wide 4-core fiber. In *Optica Optical Fiber Communications Conference and Exhibition (OFC)*, 2021.

[57] Fabian Rauscher, Andreas Kogler, Jonas Juffinger, and Daniel Gruss. IdleLeak: Exploiting Idle State Side Effects for Information Leakage. In *Network and Distributed System Security (NDSS) Symposium*, 2024.

[58] Vera Rimmer, Davy Preuveneers, Marc Juarez, Tom Van Goethem, and Wouter Joosen. Automated website fingerprinting through deep learning. In *Network and Distributed System Security (NDSS) Symposium*, 2017.

[59] Gururaj Saileshwar, Christopher W Fletcher, and Moinuddin Qureshi. Streamline: a fast, flushless cache covert-channel attack by enabling asynchronous collusion. In

ACM International Conference on Architectural Support for Programming Languages and Operating Systems (ASPLOS), 2021.

[60] Gregg Schudel and David Smith. *Router security strategies: Securing IP network traffic planes*. Pearson Education. 978-1-58705-336-8, 2007.

[61] Michael Schwarz, Daniel Gruss, Samuel Weiser, Clémentine Maurice, and Stefan Mangard. Malware Guard Extension: Using SGX to Conceal Cache Attacks. In *SIG SIDAR Conference on Detection of Intrusions and Malware & Vulnerability Assessment (DIMVA)*, 2017.

[62] Michael Schwarz, Clémentine Maurice, Daniel Gruss, and Stefan Mangard. Fantastic Timers and Where to Find Them: High-Resolution Microarchitectural Attacks in JavaScript. In *Financial Cryptography and Data Security (FC)*, 2017.

[63] Michael Schwarz, Martin Schwarzl, Moritz Lipp, Jon Masters, and Daniel Gruss. NetSpectre: Read Arbitrary Memory over Network. In *European Symposium on Research in Computer Security (ESORICS)*, 2019.

[64] Tanvi Sharma. Controlling Queue Delay (CoDel) to counter the Bufferbloat Problem in Internet. *International Journal of Current Engineering and Technology*, 4(3):2210–2215, 2014.

[65] Meng Shen, Zhenbo Gao, Liehuang Zhu, and Ke Xu. Efficient fine-grained website fingerprinting via encrypted traffic analysis with deep learning. In *International Symposium on Quality of Service (IWQOS)*, 2021.

[66] Meng Shen, Yiting Liu, Liehuang Zhu, Xiaojiang Du, and Jiankun Hu. Fine-grained webpage fingerprinting using only packet length information of encrypted traffic. *IEEE Transactions on Information Forensics and Security (TIFS)*, 16:2046–2059, 2020.

[67] Meng Shen, Mingwei Wei, Liehuang Zhu, and Mingzhong Wang. Classification of encrypted traffic with second-order markov chains and application attribute bigrams. *IEEE Transactions on Information Forensics and Security (TIFS)*, 12(8):1830–1843, 2017.

[68] Meng Shen, Jinpeng Zhang, Ke Xu, Liehuang Zhu, Jiangchuan Liu, and Xiaojiang Du. Deepqoe: Real-time measurement of video qoe from encrypted traffic with deep learning. In *International Symposium on Quality of Service (IWQoS)*, 2020.

[69] Meng Shen, Jinpeng Zhang, Liehuang Zhu, Ke Xu, and Xiaojiang Du. Accurate decentralized application identification via encrypted traffic analysis using graph neural networks. *IEEE Transactions on Information Forensics and Security (TIFS)*, 16:2367–2380, 2021.

[70] Saurabh Shintre, Virgil Gligor, and João Barros. Optimal strategies for side-channel leakage in FCFS packet schedulers. In *International Symposium on Information Theory (ISIT)*, 2015.

[71] Monika Skowron, Artur Janicki, and Wojciech Mazurczyk. Traffic fingerprinting attacks on internet of things using machine learning. *IEEE Access*, 8:20386–20400, 2020.

[72] Dawn Xiaodong Song, David Wagner, and Xuqing Tian. Timing Analysis of Keystrokes and Timing Attacks on SSH. In *USENIX Security Symposium (USENIX Security)*, 2001.

[73] Andrei Tatar, Radhesh Krishnan, Elias Athanasopoulos, Cristiano Giuffrida, Herbert Bos, and Kaveh Razavi. Throwhammer: Rowhammer Attacks over the Network and Defenses. In *USENIX Annual Technical Conference (ATC)*, 2018.

[74] Vincent F Taylor, Riccardo Spolaor, Mauro Conti, and Ivan Martinovic. Robust smartphone app identification via encrypted network traffic analysis. *IEEE Transactions on Information Forensics and Security (TIFS)*, 13(1):63–78, 2017.

[75] Bjørn Ivar Teigen, Kai Olav Ellefsen, Tor Skeie, and Jim Torresen. Known Performance Issues Are Prevalent in Consumer WiFi Routers. In *International Conference on Network and Service Management (CNSM)*, 2021.

[76] Tom Van Goethem, Christina Pöpper, Wouter Joosen, and Mathy Vanhoef. Timeless Timing Attacks: Exploiting Concurrency to Leak Secrets over Remote Connections. In *USENIX Security Symposium (USENIX Security)*, 2020.

[77] Pepe Vila and Boris Köpf. Loophole: Timing Attacks on Shared Event Loops in Chrome. In *USENIX Security Symposium (USENIX Security)*, 2017.

[78] Shuochao Yao, Ailing Piao, Wenjun Jiang, Yiran Zhao, Huajie Shao, Shengzhong Liu, Dongxin Liu, Jinyang Li, Tianshi Wang, Shaohan Hu, et al. Stfnets: Learning sensing signals from the time-frequency perspective with short-time fourier neural networks. In *The World Wide Web Conference*, 2019.

[79] Yuval Yarom and Katrina Falkner. Flush+Reload: a High Resolution, Low Noise, L3 Cache Side-Channel Attack. In *USENIX Security Symposium (USENIX Security)*, 2014.

Appendix

Table 3 shows the F_1 score for each website in the top-100 open-world fingerprinting attack from Section 7.

Table 3: Websites used in the top-100 open-world fingerprinting attack and their corresponding F_1 scores.

#	Website	F_1 [%]	#	Website	F_1 [%]	#	Website	F_1 [%]
001	google.com	31	035	office.com	88	069	amazon.co.jp	69
002	youtube.com	95	036	t.co	6	070	google.co.in	32
003	baidu.com	31	037	naver.com	61	071	msn.cn	90
004	bilibili.com	52	038	apple.com	77	072	tencent.com	51
005	facebook.com	66	039	sina.com.cn	50	073	freepik.com	66
006	qq.com	63	040	aliexpress.com	85	074	etsy.com	71
007	twitter.com	82	041	yahoo.co.jp	9	075	amazon.co.uk	63
008	zhihu.com	85	042	xhamster.com	64	076	imgur.com	80
009	wikipedia.org	8	043	paypal.com	75	077	jianshu.com	5
010	amazon.com	54	044	spankbang.com	45	078	ilovepdf.com	68
011	instagram.com	85	045	pinterest.com	83	079	twitch.tv	80
012	linkedin.com	38	046	mail.ru	81	080	atlassian.net	87
013	reddit.com	64	047	ebay.com	71	081	force.com	58
014	whatsapp.com	72	048	douban.com	70	082	dropbox.com	83
015	openai.com	90	049	msn.com	94	083	office365.com	47
016	yahoo.com	53	050	imdb.com	76	084	alipay.com	5
017	bing.com	66	051	amazon.in	65	085	discord.com	85
018	taobao.com	14	052	netflix.com	83	086	namu.wiki	50
019	163.com	49	053	telegram.org	71	087	t.me	63
020	yandex.ru	80	054	dzen.ru	78	088	wordpress.com	64
021	xvideos.com	61	055	quora.com	33	089	tradingview.com	87
022	live.com	78	056	stackoverflow.com	59	090	avito.ru	70
023	pornhub.com	64	057	sohu.com	21	091	3dmgame.com	73
024	microsoft.com	72	058	spotify.com	100	092	xiaohongshu.com	55
025	vk.com	93	059	aliyun.com	93	093	instructure.com	88
026	zoom.us	84	060	xnxx.com	50	094	onlyfans.com	88
027	github.com	83	061	1688.com	47	095	amazonaws.com	8
028	jd.com	44	062	myshopify.com	54	096	flipkart.com	68
029	weibo.com	71	063	tmall.com	19	097	hao123.com	28
030	google.com.hk	13	064	indeed.com	69	098	alibaba.com	67
031	tiktok.com	91	065	deepl.com	69	099	cnki.net	12
032	canva.com	66	066	pixiv.net	92	100	mediafire.com	52
033	csdn.net	62	067	feishu.cn	66	101	other	53
034	fandom.com	70	068	duckduckgo.com	88			